Attractin/Mahogany/Zitter plays a critical role in myelination of the central nervous system

Takashi Kuramoto*†, Kazuhiro Kitada‡, Toshihide Inui§, Yoshifumi Sasaki§, Kazumi Ito¶, Takao Hase‖, Saburo Kawagachi‖, Yoshihiro Ogawa, Kazuwa Nakao**, Gregory S. Barsh††, Minako Nagao*, Toshikazu Ushijima*, and Tadao Serikawa‡**

*Carcinogenesis Division, National Cancer Center Research Institute, Chuo-ku, Tokyo 104-0045, Japan; ‡Institute of Laboratory Animals, ‖Department of Integrative Brain Science, and **Department of Medicine and Clinical Science, Graduate School of Medicine, Kyoto University, Sakyo-ku, Kyoto 606-8501, Japan; §Safety Research Laboratory, Tanabe Seiyaku Co. Ltd., Yodogawa-ku, Osaka 532-8505, Japan; ¶YS New Technology Institute, Ishibashi-machi, Tochigi 329-0512, Japan; and ††Department of Pediatrics and Genetics and the Howard Hughes Medical Institute, Stanford University School of Medicine, Stanford, CA 94305-5428

Edited by Richard L. Sidman, Harvard Medical School, Southborough, MA, and approved November 3, 2000 (received for review October 2, 2000)

The rat zitter (*zi*) mutation induces hypomyelination and vacuolation in the central nervous system (CNS), which result in early-onset tremor and progressive flaccid paresis. By positional cloning, we found a marked decrease in Attractin (*Atrn*) mRNA in the brain of the *zi*/*zi* rat and identified *zi* as an 8-bp deletion at a splice donor site of *Atrn*. *Atrn* has been known to play multiple roles in regulating physiological processes that are involved in monocyte–T cell interaction, *agouti*-related hair pigmentation, and control of energy homeostasis. Rat *Atrn* gene encoded two isoforms, a secreted and a membrane form, as a result of alternative splicing. The *zi* mutation at the *Atrn* locus darkened coat color when introduced into agouti rats, as also described in mahogany (*mg*) mice, carrying the homozygous mutation at the *Atrn* locus. Transgenic rescue experiments showed that the membrane-type *Atrn* complemented both neurological alteration and abnormal pigmentation in *zi*/*zi* rats, but that the secreted-type *Atrn* complemented neither mutant phenotype. Furthermore, we discovered that *mg* mice exhibited hypomyelination and vacuolation in the CNS associated with body tremor. We conclude from these results that the membrane *Atrn* has a critical role in normal myelination in the CNS and would provide insights into the physiology of myelination as well as the etiology of myelin diseases.

The zitter rat was found in a colony of Sprague–Dawley rats as a tremorous mutant, and subsequent genetic analysis showed that the abnormality was caused by an autosomal recessive gene, *zitter* (*zi*) (1, 2). The tremor develops spontaneously at 3 weeks of age, and flaccid paresis of the hind limb is observed at around 6 months of age (3). The main pathological findings are progressive hypomyelination and vacuolation in the central nervous system (CNS) (4). Hypomyelination is characterized by a significant decrease in the density of myelinated fibers and the number of myelin lamellae and is accompanied by aberrant or elongated myelin sheath formation (4). Vacuoles consist mainly of swollen astrocytic processes and enlargement of extracellular space as well as periaxonal spaces. The vacuoles are first detected in the pons and the outer thalamus at 3 weeks of age. With increasing age, vacuoles extend into the deep cortex, hippocampus, cervical spinal gray matter, and the granular layer and white matter of the cerebellum (5). However, the initiation of myelination and the fundamental structures of myelin sheaths are normal in the zitter rat. The biochemical components of myelin, such as myelin basic protein, proteolipid protein, and myelin-associated glycoprotein, are also normally expressed (5, 6). Therefore, the zitter rat is expected to provide useful tools for the study of axon–glia interaction and the assembly of myelin sheaths in the complex process of CNS myelination.

The *zi* gene has been mapped to a genomic region between IL-1β (*Il1b*) and prion protein (*Prnp*) on rat chromosome (Chr) 3q35 (3, 7). *Prnp* is known as a causative gene for spongiform encephalopathy, and it was considered as a strong candidate for *zi*. However, there were no differences in mRNA expression levels and nucleotide sequences of *Prnp* between the zitter and normal control rats. Thus, *Prnp* was excluded as a candidate for *zi* (7, 8). A comparative map between rat, mouse, and human showed that rat 3q35 corresponds to mouse Chr 2(70–80 cM) and human Chr 2q14 and Chr 20pter-p13 (9), but no obvious candidate genes are present in these regions.

Here we will describe the identification of *zi* by positional cloning and subsequent transgenic rescue experiments and assessment of the neurological phenotypes of Attractin (*Atrn*) mutant, mahogany (*mg*) mice. Our results show that the *Atrn* locus product has multiple functions not only in immune response, hair pigmentation, and energy control, but also in myelination in the CNS.

Materials and Methods

Genetic Fine Mapping. (WTC × WTC.ZI-*zi*/*zi*)F_1(*zi*/+) female rats were backcrossed to male WTC.ZI-*zi*/*zi* homozygote rats and intercrossed to male *zi*/+ F_1 rats to produce progeny for fine mapping of *zi*. Homozygote *zi*/*zi* animals were identified on the basis of appearance of tremor at 3–4 weeks of age. Simple sequence length polymorphisms (SSLPs) at *Il1b* and *Prnp* were genotyped as described (3, 7). Three gene-specific SSLP markers, *D3Kur2*/*Ptpns1*, *D3Kur7*/*Ptpra*, and *D3Kur55*/*Sn*, were developed from the published sequences (GenBank accession numbers D85183, Z36293, and L01702), and two SSLP markers, *D3Kur1*/*Pdyn* and *D3Kur9*/*Oxt*, were developed from the cosmid clones as described (10). While the physical map was assembled (see below), seven anonymous SSLP markers, *D3Kur4*, *D3Kur20*, *D3Kur24*, *D3Kur30*, *D3Kur34*, *D3Kur37*, and *D3Kur40*, were developed from rat cosmid and P1 clones.

Physical Mapping. A rat P1 library was screened at IncyteGenomics (Palo Alto, CA) by hybridizing with DNA fragments amplified by *D3Kur7*/*Ptpra*, *D3Kur12*/*Oxt*, *D3Kur14*, *D3Kur18*, *D3Kur21*, *D3Kur27*, and *D3Kur33* (Fig. 1*b*). A rat P1-derived

This paper was submitted directly (Track II) to the PNAS office.

Abbreviations: *Atrn*, Attractin; *zi*, zitter; *mg*, mahogany; CNS, central nervous system; Chr, chromosome; EST, expressed sequence tag; EMG, electromyogram; *Prnp*, prion protein gene; SSLP, simple sequence length polymorphism; PAC, P1-derived artificial chromosome; STS, sequence tagged site; MMT, mouse metallothionein; CAG, chicken β-actin.

Data deposition: The rat *Atrn* cDNA and exon sequences reported in this paper have been deposited in the GenBank database (accession nos. AB038387, AB038388, and AB049222–AB049248). The oligonucleotide sequences for the STS markers developed in this study are available at http://www.ncc.go.jp/research/rat-genome.

†To whom reprint requests should be addressed at: Carcinogenesis Division, National Cancer Center Research Institute 5-1-1, Tsukiji, Chuo-ku, Tokyo 104-0045, Japan. E-mail: tkuramot@gan2.ncc.go.jp.

The publication costs of this article were defrayed in part by page charge payment. This article must therefore be hereby marked "*advertisement*" in accordance with 18 U.S.C. §1734 solely to indicate this fact.

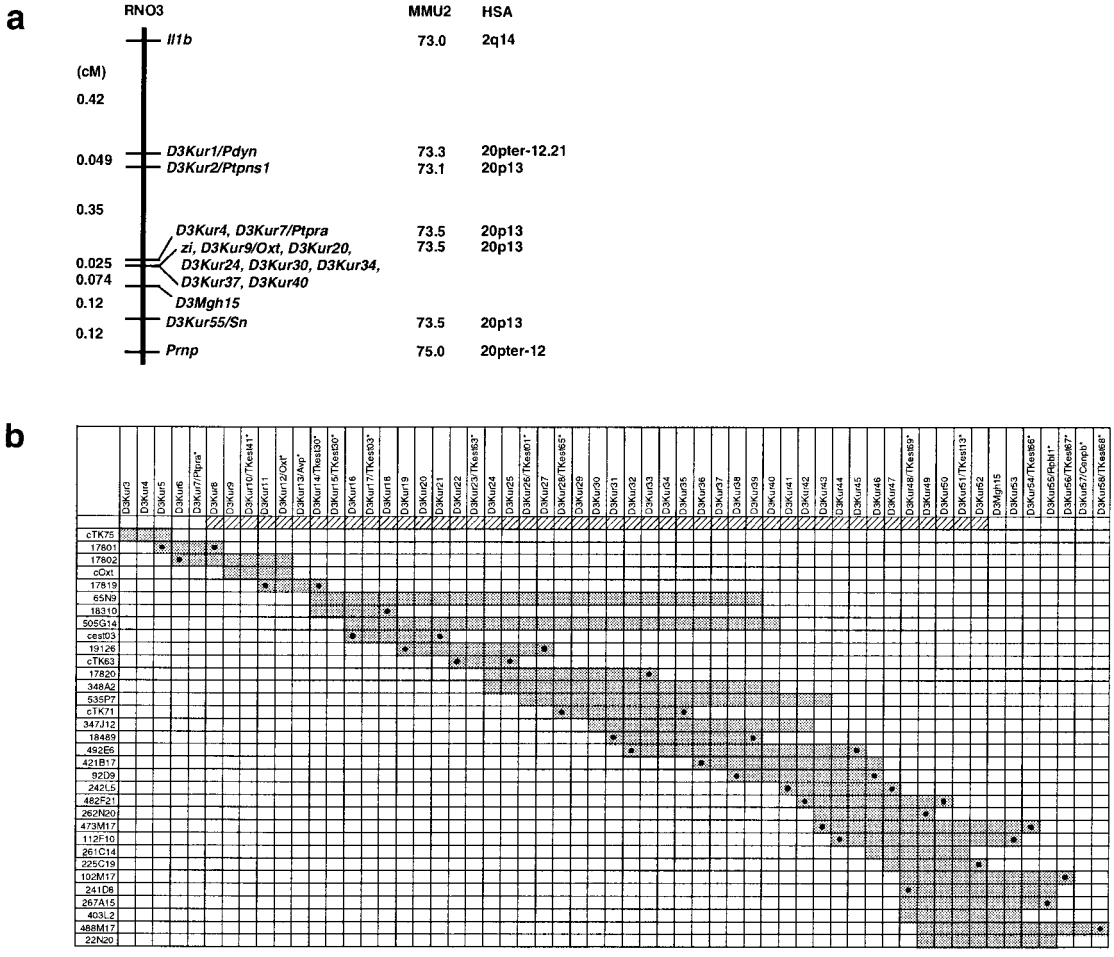

Fig. 1. Genetic linkage map and a contig of the *zi*-critical region. (*a*) The genetic linkage map of the region surrounding the *zi* locus. For loci also mapped in mouse and human, their locations in the corresponding chromosomes are indicated on their right. (*b*) The contig spanning the *zi*-critical region. Cosmid, P1, and PAC clones are listed on the left; STS markers are listed at the top. PCR signals on clones are indicated by dark gray boxes. The *zi*-critical region is depicted by oblique lines. PCR signals of the markers derived from end sequences are indicated by closed circles on the corresponding clones. Asterisks at the top show transcribed sequences. Cosmid clones are indicated by the addition of "c" to their names. P1 clones are indicated by five-digit numbers given by IncyteGenomics.

artificial chromosome (PAC) library was screened by hybridizing with DNA fragments amplified by *D3Kur39*, *D3Kur44*, and *D3Kur50*. Isolated clones were subjected to sequencing of their ends, and the sequences were used to design the PCR primers for sequence tagged site (STS) markers after repeat sequences were masked. To determine the precise physical positions of STS and SSLP markers as well as clone overlap and orientation, STS content mapping was performed by PCR with genomic clone DNA templates. Comparative mapping was performed by searching the database for genes or expressed sequence tags (ESTs) mapped to human Chr 20pter-p12 and mouse Chr 2, and by mapping them in the contig. BLAST homology searches were made by using the repeat-masked end sequences.

Cloning of Rat *Atrn* cDNA. A rat brain cDNA library was constructed in λMOSElox (Amersham Pharmacia) and screened with a rat probe corresponding to nucleotides 50–437 of KIAA0548, the partial sequence of the human attractin (*ATRN*) gene (11). To obtain the 5′ part of the cDNA and the 3′ part of the short form of the rat *Atrn* gene, rapid amplifications of cDNA ends were conducted with the use of Marathon-Ready cDNA (CLONTECH).

Determination of Exon–Intron Boundaries of the *Atrn* Gene. A shotgun library was constructed from PAC 473M17 containing the entire rat *Atrn* gene and screened with the rat *Atrn* cDNA. Intron–exon boundaries were defined either by sequencing of the isolated clones or by direct sequencing of the PAC with the use of the *Atrn* cDNA-specific primers. Introns were amplified by PCR with *LA-Taq* DNA polymerase (Takara Shuzo, Kyoto, Japan), with the PAC as a template, and their lengths were assessed by electrophoresis. The exon–intron boundaries were verified by direct sequencing of the PCR products.

Genotyping of *Agouti* and *Atrn*. Genotypes at loci *agouti* (*a*) and *Atrn* of the F_2 animals were determined by an SSLP marker in intron 2 of rat *agouti* (5′-GGGAAAGACCATAGCTGCTA-3′ and 5′-AATAACAGCCTGGGAAAATG-3′) and by the marker detecting the 8-bp deletion of the *zi*-allele of *Atrn* (5′-GGAGTTGGCAACTGAAGAAC-3′ and 5′-GAAAGGGCAGAGACAAAGTT-3′).

Transgenic Rescue Experiment. A 4.4-kb cDNA fragment containing the coding sequence for a membrane type of *Atrn* and a 3.9-kb cDNA fragment for a secreted type were subcloned into pBluescriptII (Stratagene). Wild-type *Atrn* transgenes were constructed with the use of the cDNA fragment, the mouse metallothionein (MMT) promoter, or the modified chicken β-actin (CAG) promoter with cytomegalovirus immediate early enhancer (12), and a ≈500-bp fragment containing the simian virus

Table 1. Genes/ESTs mapped to the contig constructed in this study

Locus symbol*	STS maker	Method†	Origin	UniGene	Description
Ptpra	*D3Kur7*	C	STS-WI-8798	Hs.26045	Protein-tyrosine phosphatase, receptor-type, alpha (OMIM#176884)
TKest41	*D3Kur10*	E	BAC179P17-M13F‡	Mm.30057	ESTs
Oxt	*D3Kur12*	C		Hs.113216	Oxytocin (OMIM#167050)
Avp	*D3Kur13*	C		Hs.89648	Arginine vasopressin (OMIM#192340)
TKest30	*D3Kur15*	C and E	STS-stSG4244 and P1-17819-T7	Hs.26009	KIAA0860 protein, complete cds
TKest03	*D3Kur17*	C	STS-A005R07	Hs.90232	KIAA0552 protein, complete cds
TKest63	*D3Kur23*	E	BAC173P11-M13F‡	Mm.21399	ESTs, Highly similar to HAM1 protein (*Saccharomyces cerevisiae*)
TKest01	*D3Kur26*	C	STS-stSG3058	Rn.6943	ESTs
TKest65	*D3Kur28*	E	Cosmid-TK71-M13F	Mm.35506	ESTs
TKest69	*D3Kur48*	E	PAC241D8-SP6	Rn.22428	ESTs
TKest13	*D3Kur51*	C	STS-A005O05	Hs.194019	KIAA0548 protein, partial cds
TKest66	*D3Kur54*	E	PAC473M17-SP6	Not assigned	EST from normalized rat spleen, cDNA clone RSPBR15 (AI013648)
Rpl12	*D3Kur55*	E	PAC267A15-T7	Hs.182979	Ribosomal protein L12 (OMIM#180475)
TKest67	*D3Kur56*	E	PAC102M17-T7	Rn.39027	ESTs
Cenpb	*D3Kur57*	C	STS-Bdyc4e10	Hs.85004	Centromeric protein B (OMIM#117140)
TKest68	*D3Kur58*	E	PAC488M17-SP6	Rn.41637	EST

*Ordered according to map position from proximal (top) to distal (bottom).
†C, comparative mapping; E, end sequence and BLAST homology search.
‡Derived from a bacterial artificial chromosome contig spanning the mouse syntenic region of the *zi* locus (T.K., unpublished result).

40 poly(A) signal derived from pEVBHis (Invitrogen). The transgene was microinjected into the pronuclei of fertilized oocytes collected from Wistar rats, and the eggs subsequently were transferred to recipients. The (Founder rats × WTC.ZI-*zi*/*zi*)F_1 (*zi*/+, *tg*/−) rats were backcrossed with WTC.ZI-*zi*/*zi* rats to obtain *zi*/*zi* homozygous rats carrying the transgene (*zi*/*zi*, *tg*/−). Transgenic rats were identified by PCR analysis of genomic DNA isolated from tail biopsies. The copies of the transgene on autoradiograph normalized relative to endogenous *Atrn* gene were quantified with computerized image display system BAS2000 (Fuji Film, Tokyo).

Histopathological and Electromyogram (EMG) Analysis of *mg* Mice. Histopathological analysis of C3H/HeJ-mg^{3J}/mg^{3J} mice was carried out at 40 days of age. Light microscopic observations of brain and spinal cord (cervical enlargement) and electron microscopic observations of thalamus and midbrain were performed as described (13). EMG recordings were performed at 3 weeks of age. Intramuscular EMG electrodes were acutely implanted in the quadriceps and hamstring muscles of the right hind limbs. EMGs were recorded within a bandwidth of 100–1,500 Hz and analyzed with a Signal Averager (Cambridge Electronic Design, Cambridge, U.K.).

Results

Genetic and Physical Maps of the *zi*-Critical Region. A total of 3,104 backcross and 474 intercross animals were produced, and their genotype at the *zi* locus was determined by examining the presence of tremor. Thirty-five backcross and 12 intercross animals carried a recombinant chromosome between *Il1b* and *Prnp*. Genetic linkage study of these informative animals, using the five gene-specific and seven anonymous markers developed in this study, narrowed down *zi* to a 0.1-cM interval between *D3Kur7*/*Ptpra* and *D3Mgh15*, which corresponded to human Chr 20p13 and mouse Chr 2(73.5) (Fig. 1*a*). The *zi* gene showed no recombination with *D3Kur9*/*Oxt*, *D3Kur20*, *D3Kur24*, *D3Kur30*, *D3Kur34*, *D3Kur37*, and *D3Kur40* in 4,052 informative meioses.

A rat P1 library was initially screened with *D3Kur7*/*Ptpra* and *D3Kur12*/*Oxt*. After the subsequent chromosomal walking with the P1 library and a rat PAC library and aligning them by STS content mapping with the use of 57 markers developed in this study, a contig that comprised five cosmid, seven P1, and 21 PAC clones and covered *D3Kur3-D3Kur7*/*Ptpra-D3Mgh15-D3Kur58* was constructed. Transcripts in the contig were identified by comparative mapping and end sequencing of the constituent large-insert clones. Taking advantage of the large conserved syntenic region between rat Chr 3 and human Chr 20p, 62 genes/ESTs known to be located on human chromosome 20pter-p12 were tested, and four known genes (*Avp*, *Cenpb*, *Oxt*, and *Ptpra*) and four ESTs were localized in the contig (Table 1). With a BLAST homology search using 56 end sequences, one gene, *Rpl12*, and eight ESTs were found in the contig. Because an EST (*TKest30*) was commonly identified by the comparative mapping and the end sequencing, a total of 16 genes/ESTs were mapped in the contig (Fig. 1*b* and Table 1). Among the 16 genes/ESTs identified in the contig, 10 were localized in the *zi*-critical region.

Reduction of *Atrn* Expression in Zitter Rats. Expression levels of the 10 genes/ESTs in the *zi*-critical region were analyzed by Northern blot analysis. It was revealed that the expression of an EST, *TKest13*, was markedly reduced in WTC.ZI-*zi*/*zi* rats, although faint multiple bands of 8–10 kb were observed (Fig. 2*a*). The other nine genes/ESTs showed the same levels of expression in WTC and WTC.ZI-*zi*/*zi* rats, and no nucleotide differences resulted in amino acid changes specific to *zi*/*zi* rats. By a database search, *TKest13* proved to be the *KIAA0548*, which is a part of the membrane type of the human *ATRN* gene.

Isoforms and Exon–Intron Organization of the Rat *Atrn* Gene. In the brain of WTC rats, two kinds of transcripts with sizes of 9.0 kb and 4.5 kb were observed. We cloned the two transcripts and determined their nucleotide sequences (GenBank accession numbers AB038387 and AB038388). We also determined the exon–intron boundaries and the lengths of introns of the rat *Atrn* gene. It spanned over 120 kb and contained at least 29 exons (Fig. 3*a*). The 4.5-kb transcript was found to be generated by an alternative splicing, skipping a splice donor site in intron 24, and using a stop codon and a polyadenylation signal in the intron (Fig. 3*b*).

The 9.0-kb transcript was deduced to encode a 1,432-aa polypeptide, which corresponded to the membrane-type human *ATRN* locus product. Rat membrane type showed 93% and 97% homology with human and mouse *Atrn* product, respectively. The 4.5-kb transcript was deduced to encode a 1,276-aa polypep-

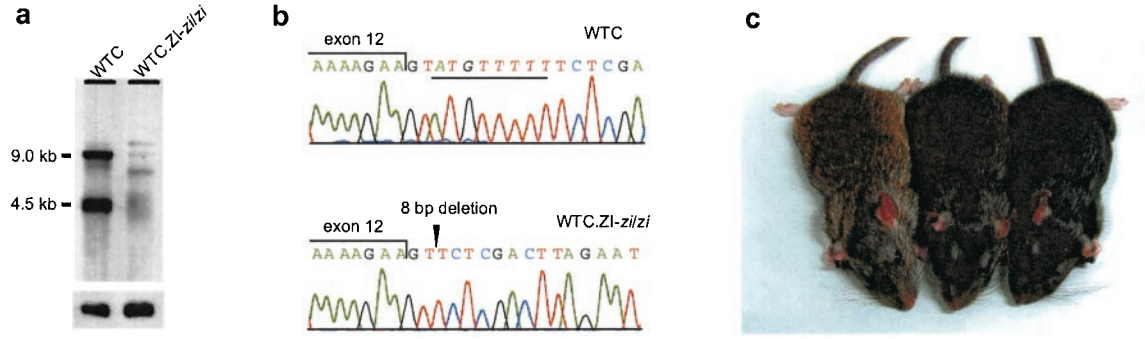

Fig. 2. *Zi* mutation at rat *Atrn* gene. (*a*) Northern blot analysis of *Atrn* in the brains of WTC and WTC.ZI-*zi*/*zi* rats. A marked reduction of *Atrn* expression was observed in *zi*/*zi* rats. Hybridization signals of β-actin on the same blot are shown below. (*b*) Sequencing analysis of the splice donor site of the *Atrn* intron 12 in WTC (*Upper*) and WTC.ZI-*zi*/*zi* (*Lower*). An 8-bp deletion was identified in *zi*/*zi* rats (underlined in the *Upper* and shown with an arrowhead in the *Lower*) and was expected to result in an abnormal splicing. (*c*) Effect of the *zi* allele on coat color in rats. The agouti rat homozygous for the *zi* allele of *Atrn* (center) was more darkly pigmented than the agouti rat without the *zi* allele (*Left*) but less pigmented than nonagouti rat homozygous for the *zi* alleles (*Right*).

tide, which shared 1,271 N-terminal amino acid residues with the product of the 9.0-kb transcript, had five unique C-terminal residues, and did not have the transmembrane domain. It corresponded to the secreted type of the human *ATRN* locus product, although this secreted type is not observed in mice. Both polypeptides were predicted to contain four epidermal growth factor domains, a CUB domain, and C-type lectin domain (Fig. 3*c*).

A Splice Site Mutation in *Atrn* in Zitter Rats. The entire coding region and all of the exon-intron boundaries of *Atrn* were sequenced in WTC.ZI-*zi*/*zi* rats. An 8-bp deletion at the splice donor site of intron 12 was identified (Fig. 2*b*), which was expected to result in aberrant and unstable transcripts. There were no other nucleotide differences between WTC and WTC.ZI-*zi*/*zi* rats.

Effect of the *zi* Mutation on Coat Color. To examine the effect of the *zi*-allele of *Atrn* on coat color (see *Discussion*), the mutant allele

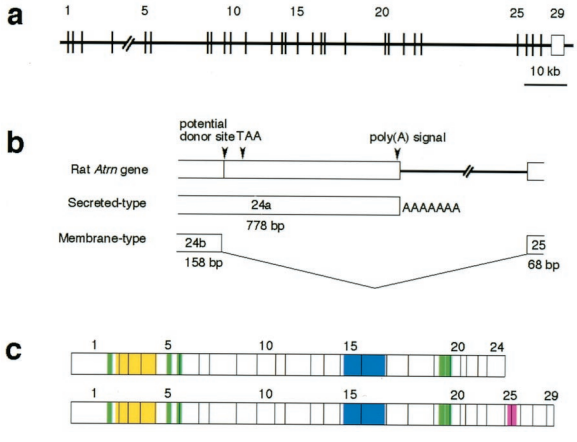

Fig. 3. Rat *Atrn* gene and its transcripts. (*a*) Exon–intron organization of the rat *Atrn* gene. The gene comprises at least 29 exons and 28 introns, which are represented as boxes and lines. The length of intron 4 could not be determined. (*b*) Alternative splicing at exon 24 of the rat *Atrn* gene: genome organization around intron 24 (*Top*). The secreted-type *Atrn* transcript used the stop codon (TAA) and the poly(A) addition signal located within intron 24 (*Middle*). The membrane-type *Atrn* transcript was spliced at the potential donor site located 15 bp upstream from the stop codon of the secreted-type *Atrn* (*Bottom*). (*c*) *Atrn* transcripts for the secreted type (*Upper*) and membrane type (*Lower*). Five epidermal growth factor-related domains (green), a CUB domain (yellow), and c-type lectin (blue) are common in the two isoforms, but a transmembrane domain (red) is found only in the membrane type.

was brought into a nonalbino background by producing F_2 intercross rats from ACI/N (*A*/*A*, +/+) and WTC.ZI-*zi*/*zi* (*a*/*a*, *zi*/*zi*, albino). Ten genotyped nonalbino agouti rats homozygous for the *zi* allele of *Atrn* were recovered from the 115 F_2 rats, and all of them showed a darker coat color than the agouti rats without the *zi* allele (Fig. 2*c*).

Transgenic Rescue. To confirm that *Atrn* is *zi* itself, and to clarify which transcript is responsible for the neuropathological phenotypes in zitter rats, we carried out transgenic rescue experiments. The wild-type transcript for the membrane type was placed under the control of a CAG promoter or MMT promoter (CAG + M, MMT + M), and the secreted type was placed under the control of MMT promoter (MMT + S). Six independent transgenic lines, two lines for each construct, were established (Table 2). Southern blot analysis demonstrated that five of the six lines carried a single copy of the transgene, and one line carried approximately 100 copies. Northern blot analysis with a probe specific for the membrane-type transcript detected 9.0-kb endogenous and 4.9-kb transgene-specific transcripts in the brain of CAG + M and MMT + M lines (Fig. 4*a*). A probe specific for the secreted-type transcript detected 4.5-kb endogenous and 4.4-kb transgene-specific transcripts in the brain of CAG + S lines (Fig. 4*a*).

All of the 38 transgenic *zi*/*zi* rats in N2 progeny of TK320-14, TK320-27, TK322-43, and TK322-48 lines were completely rescued from body tremor, aberrant myelination, and vacuolations in the CNS (Fig. 4*b*). They showed no flaccid paresis at 6 months of age. On the other hand, TK328-73 and TK328-76 lines failed to be rescued from tremor, hypomyelination, or vacuolation of the CNS. Thus, the zitter neuropathological phenotypes were complemented in all lines expressing the membrane-type transgene but not the secreted-type transgene (Table 2). Furthermore, the membrane type also rescued darkly pigmented coat color phenotypes but not the secreted type (Table 2).

Neurological Alterations in *mg* Mice. Light microscopic observation of the CNS of mg^{3J}/mg^{3J} mice revealed vacuole formation that was widely distributed in the brainstem, cerebral cortex, cerebellum, and spinal cord. The vacuoles were well delineated and circular, and their sizes were variable, some reaching up to 10–20 μm in diameter. In Epok 812 sections stained with toluidine blue, aberrant myelin sheaths and vacuoles surrounded by myelin were identified (Fig. 5*a*). Electron microscopic observation revealed that some vacuoles contained vacuolar membranous structures, which were considered to be degenerate organelles. Such vacuoles were regarded as swollen processes of neurons or glial cells. In addition, elongated redundant myelin sheaths and scroll-like

Table 2. Phenotypes of *zi*/*zi* rats in *Atrn*-transgenic lines

Line	Transgene		Number of N2 animals examined	Phenotypes		
	Name	Number of copy		Symptoms	CNS pathology	Coat color
TK320-14	CAG+M	~1	6	Normal	Normal	Agouti
TK320-27	CAG+M	~1	10	Normal	Normal	Agouti
TK322-43	MMT+M	~1	8	Normal	Normal	Agouti
TK322-48	MMT+M	~1	8	Normal	Normal	Agouti
TK328-73	MMT+S	~100	5	Tremor, paresis	Vacuolation, hypomyelination	Mahogany
TK328-76	MMT+S	~1	5*	Tremor, paresis	Vacuolation, hypomyelination	Mahogany

*N3 animals were included.

structures were identified among the myelinated axons (Fig. 5*b*). The distribution and morphology of vacuoles and aberrant myelin sheaths are very similar to those observed in the zitter rats (4–6).

Examination of mg^{3J}/mg^{3J} mice allowed us to detect slight body tremor after weaning that occurred sporadically at rest and, more often, a few seconds before locomotion. The tremor was confirmed by EMGs showing strong and reciprocal bursts of activity in both the quadriceps and the hamstring muscles at a fairly constant rate (Fig. 5*c*). The tremor frequency was approximately 17 Hz.

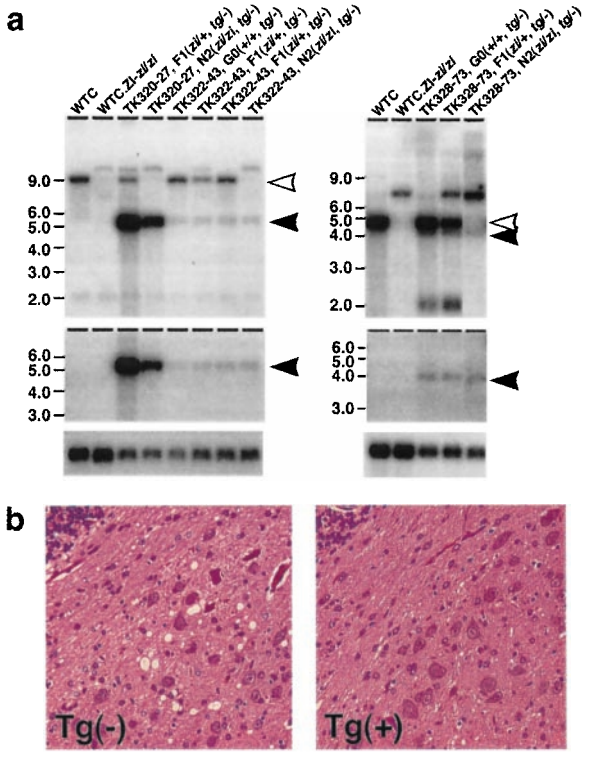

Fig. 4. Transgenic rescue from zitter neuropathological phenotypes by introduction of the wild-type *Atrn* gene. (*a*) Expression of transgene assessed by Northern blot analysis. Poly(A) RNAs from WTC, WTC.ZI-*zi*/*zi*, TK320-27, TK322-43, and TK328-73 are probed with membrane-type *Atrn* (*Top, Left*) and secreted-type *Atrn* (*Top, Right*). The membrane-type *Atrn*-specific probe detected 9.0-kb endogenous (open arrowhead) and 4.9-kb transgene (closed arrowhead) transcripts (*Left*). The secreted-type *Atrn*-specific probe detected 4.5-kb endogenous (open arrowhead) and 4.4-kb transgene (closed arrowhead) transcripts (*Right*). A DNA fragment containing simian virus 40 poly(A) additional signal only detected the transgene-specific transcripts indicated by closed arrowheads (*Middle*). Hybridization signals of β-actin on the same blot are shown at the bottom. (*b*) Sagittal section of cerebellum nuclei of *zi*/*zi* rats from a TK320–27 transgenic line with the transgene (*Right*) or without the transgene (*Left*). Note that the Tg(−) cerebellum exhibits vacuolation, whereas the Tg(+) cerebellum is restored.

Discussion

In this study, we found a marked reduction of secreted- and membrane-type *Atrn* transcripts in the brain of the zitter rat. The 8-bp deletion we found at the splice donor site of intron 12 of *Atrn* was expected to result in unstable transcripts, and the deletion was considered to be the causative mutation for the abnormalities observed in the zitter rat. Transgenic study demonstrated that only the membrane-type transgene can rescue the neurological abnormalities and coat color of the zitter rat. We also demonstrated that the mg^{3J}/mg^{3J} mice, which carried a 5-bp deletion in the coding sequence of *Atrn*, showed body tremor and histopathological abnormalities similar to those of the zitter rat. These results conclude that the membrane-type *Atrn* locus product, but not the secreted type, is responsible for the zitter mutant phenotypes observed in this study, including hypomyelination and vacuolation in the CNS and hair pigmentation.

Functions of the *Atrn* locus products have been investigated from immunological studies in human and analysis of the mouse

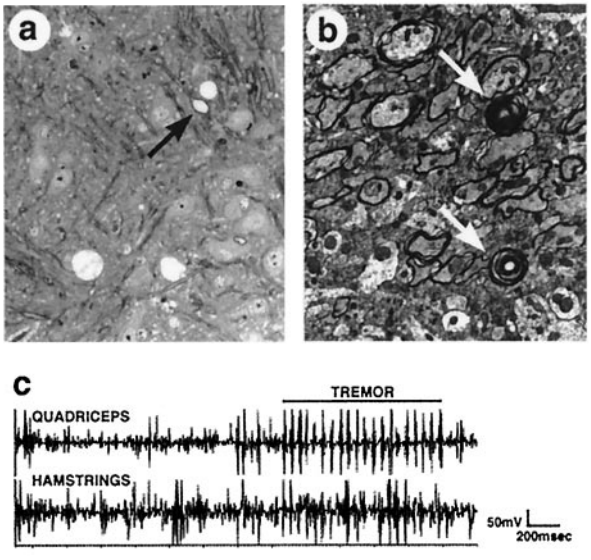

Fig. 5. Neurological abnormalities of C3H/HeJ-mg^{3J}/mg^{3J} mice. (*a*) An Epok 812 semithin section of the mesencephalic tegmentum. Vacuoles were formed in neuropil. They appeared to be empty, and some of them were surrounded by myelin (arrow) (toluidine blue staining, ×600). (*b*) An electron micrograph of the thalamus. Aberrant myelin sheaths, such as scroll-like structures (white arrows), were evident among the myelinated axons (×4,500). (*c*) EMGs of C3H/HeJ-mg^{3J}/mg^{3J} mice. The horizontal bar over the EMGs indicates a tremor pattern: nearly reciprocal activation of the quadriceps and hamstring muscles at a fairly constant rate. Background irregularities presumably exhibit motor units that fired near their threshold.

coat color mutant mahogany (*mg*). The secreted-type *ATRN* locus product Attractin (ATRN) is a glycosylated serum protein and is known as a mediator of monocyte spreading and T cell clustering (14). Recently, the presence of membrane-type ATRN has been demonstrated in humans (15). In mice, only membrane-type ATRN has been observed so far, and its loss-of-function mutations are known to be the cause of *mg* mutants. The *mg* mutant mice display darkened coat color that is *agouti*-dependent and increased basal metabolic rate that is *agouti*-independent (16–18). Both the secreted-type and membrane-type ATRN contain two epidermal growth factor domains, a CUB domain, a C-type lectin domain, and two laminin-like epidermal growth factor domains (14, 17, 19). The membrane-type ATRN is thought to have these functional domains in its extracellular portion.

This study demonstrated that ATRN has a novel function in myelination, in addition to those functions in the immune response, hair pigmentation, and energy metabolism. Overlap of the CNS regions showing high *Atrn* expression with those showing severe hypomyelination and vacuolation also supports our conclusion (20). The myelination requires the coordinated synthesizing of various structural proteins and enzymes, the initial axon–glia interaction, the assembly process of the myelin sheath, and the long-term interaction of axons with myelinating glia (21). Extracellular functional domains in the membrane-type ATRN indicate that it is involved in cell adhesion and receptor–ligand interactions (22–24). These strongly suggest that membrane-type ATRN is anchored on the surface of neurons or glial cells and mediates the myelination signal through its extracellular domains.

Although the role of the membrane-type ATRN in energy metabolism has been known in mice (16), it would be difficult to evaluate its roles in rats, because basal metabolic rate cannot be measured precisely because of the presence of conspicuous tremor in zitter rats. Conversely, mg^{3J}/mg^{3J} mice exhibited slight tremor and hypomyelination and vacuolation in their CNS. Because even minimal increases in muscle tone significantly increase basal metabolic rate, an increase of basal metabolic rate in the *mg* mutant mice could be partially due to the neurological abnormalities. Although it is proposed that inhibitors of the membrane-type ATRN would be attractive candidates for drugs to prevent or reverse the most common forms of human obesity (25–27), the critical role of ATRN in myelination disclosed in this study raises great concern about this idea.

As for positional cloning in this study, the comparative mapping and end sequencing complemented each other and efficiently identified the transcription units in the *zi*-critical region. The potential of the comparative mapping approach will be appreciably expanded when the entire sequence of the human genome is determined (9). Therefore, we expect that the approach described here would be a prototype for identifying transcripts in the rat contig.

We are grateful to Dr. T. Sugimura for critical reading of the manuscript. We also thank M. Sugiyama, T. Nomoto, C. Okumura, S. Nakanishi, and K. Yamasaki for their technical assistance. This work was supported by a grant-in-aid for the second-term Cancer Control Strategy from the Ministry of Health and Welfare; a grant-in-aid from the Ministry of Education, Science, Sports, and Culture; a grant for Research on Health Sciences focusing on Drug Innovation from the Japan Health Sciences Foundation; and a grant from the Sankyo Foundation of Life Science.

1. Rehm, S., Mehraein, P., Anzil, A. P. & Deerberg, F. (1982) *Lab. Anim. Sci.* **32,** 70–73.
2. Yamada, T., Mori, M., Hamada, S., Serikawa, T. & Yamada, J. (1989) *J. Hered.* **80,** 383–386.
3. Kuramoto, T., Yamasaki, K., Kondo, A., Nakajima, K., Yamada, M. & Serikawa, T. (1998) *Exp. Anim.* **47,** 75–81.
4. Kondo, A., Nagara, H., Akazawa, K., Tateishi, J., Serikawa, T. & Yamada, J. (1991) *Brain* **114,** 979–999.
5. Kondo, A., Sendoh, S., Miyata, K. & Takamatsu, J. (1995) *J. Neurocytol.* **24,** 533–544.
6. Kondo, A., Sendoh, S., Akazawa, K., Sato, Y. & Nagara, H. (1992) *Brain Res. Dev. Brain Res.* **67,** 217–228.
7. Kuramoto, T., Mori, M., Yamada, J. & Serikawa, T. (1994) *Biochem. Biophys. Res. Commun.* **200,** 1161–1168.
8. Gomi, H., Ikeda, T., Kunieda, T., Itohara, S., Prusiner, S. B. & Yamanouchi, K. (1994) *Neurosci. Lett.* **166,** 171–174.
9. Serikawa, T., Cui, Z., Yokoi, N., Kuramoto, T., Kondo, Y., Kitada, K. & Guenet, J. L. (1998) *Exp. Anim.* **47,** 1–9.
10. Kuramoto, T., Mori, M., Hirayama, N., Saburi, S., Yamada, J. & Serikawa, T. (1993) *Acta Histochem. Cytochem.* **26,** 325–332.
11. Nagase, T., Ishikawa, K., Miyajima, N., Tanaka, A., Kotani, H., Nomura, N. & Ohara, O. (1998) *DNA Res.* **5,** 31–39.
12. Niwa, H., Yamamura, K. & Miyazaki, J. (1991) *Gene* **108,** 193–199.
13. Inui, T., Yamamura, T., Yuasa, H., Kawai, Y., Okaniwa, A., Serikawa, T. & Yamada, J. (1990) *Brain Res.* **517,** 123–133.
14. Duke-Cohan, J. S., Gu, J., McLaughlin, D. F., Xu, Y., Freeman, G. J. & Schlossman, S. F. (1998) *Proc. Natl. Acad. Sci. USA* **95,** 11336–11341.
15. Duke-Cohan, J. S., Tang, W. & Schlossman, S. F. (2000) *Adv. Exp. Med. Biol.* **477,** 173–185.
16. Dinulescu, D. M., Fan, W., Boston, B. A., McCall, K., Lamoreux, M. L., Moore, K. J., Montagno, J. & Cone, R. D. (1998) *Proc. Natl. Acad. Sci. USA* **95,** 12707–12712.
17. Nagle, D. L., McGrail, S. H., Vitale, J., Woolf, E. A., Dussault, B. J., Jr., DiRocco, L., Holmgren, L., Montagno, J., Bork, P., Huszar, D., *et al.* (1999) *Nature (London)* **398,** 148–152.
18. Miller, K. A., Gunn, T. M., Carrasquillo, M. M., Lamoreux, M. L., Galbraith, D. B. & Barsh, G. S. (1997) *Genetics* **146,** 1407–1415.
19. Gunn, T. M., Miller, K. A., He, L., Hyman, R. W., Davis, R. W., Azarani, A., Schlossman, S. F., Duke-Cohan, J. S. & Barsh, G. S. (1999) *Nature (London)* **398,** 152–156.
20. Lu, X., Gunn, T. M., Shieh, K., Barsh, G. S., Akil, H. & Watson, S. J. (1999) *FEBS Lett.* **462,** 101–107.
21. Kettenmann, H. & Ransom, B. R. (1995) *Neuroglia* (Oxford Univ. Press, New York).
22. Bork, P. & Beckmann, G. (1993) *J. Mol. Biol.* **231,** 539–545.
23. Appella, E., Weber, I. T. & Blasi, F. (1988) *FEBS Lett.* **231,** 1–4.
24. Weis, W. I., Taylor, M. E. & Drickamer, K. (1998) *Immunol. Rev.* **163,** 19–34.
25. Schwartz, M. W. (1999) *Nat. Med.* **5,** 374–375.
26. Jackson, I. J. (1999) *Trends Genet.* **15,** 429–431.
27. Dinulescu, D. M. & Cone, R. D. (2000) *J. Biol. Chem.* **275,** 6695–6698.